Enhancement of acousto-optic diffraction efficiency in SiO_2 crystals due to ellipticity of optical eigenwaves: isotropic acousto-optic interaction

Mys O., Adamenko D. and Vlokh R.

O. G. Vlokh Institute of Physical Optics, 23 Dragomanov Street, 79005 Lviv, Ukraine

Received: 29.03.2023

Abstract. Based on the analysis of influence of a natural optical activity on the efficiency of isotropic acousto-optic (AO) diffraction, it has been found that accounting for the optical activity and a nonzero ellipticity of optical eigenwaves in quartz crystals leads to a peak-like increase in the effective elasto-optic coefficients and the acousto-optic figure of merit. We have shown that the AO figure of merit for the type I of AO interactions increases by 54%, reaching the value 1.58×10^{-15} s^3/kg. In case of AO interactions of the type II, it increases by more than three times and achieves nearly the same value. A similar situation also occurs for the types III and IV of AO interactions with the acoustic wave QT_1. In particular, the peak value of the AO figure of merit for the type III of AO interactions increases by 19% and reaches 1.22×10^{-15} s^3/kg, while the AO figure of merit for the type IV of AO interactions increases more than order of magnitude (from 9.6×10^{-17} to 1.22×10^{-15} s^3/kg). The results of our study can be useful for developing the AO devices based on crystalline quartz and minimizing their energy consumption.

Keywords: acousto-optic diffraction, optical activity, quartz crystals, diffraction efficiency, ellipticity of optical eigenwaves

UDC: 535.43, 535.551, 535.562, 534-16

1. Introduction

The influence of a natural optical activity on the conditions of acousto-optic (AO) diffraction has been noted in the works [1, 2]. It has been shown that the optical activity affects the phase-matching conditions at the Brillouin scattering and the polarization of diffracted optical wave, provided that the incident light propagates along the directions close to the optic axis. It has been demonstrated in our recent work [3] that the ellipticity of optical eigenwaves can enhance essentially the efficiency of AO diffraction whenever the AO interaction takes place between the optical waves which correspond to the eigenwave polarizations in optically active crystals.

One of the examples of such enhancement is a case of TeO_2 crystals [4] where the AO figure of merit $M_2 = n_i^3 n_d^3 p_{eff}^2 / \rho v^3$ (with n_i and n_d being the refractive indices of respectively the incident and diffracted optical waves, v the velocity of an acoustic wave (AW), p_{eff} the effective elasto-optic (EO) coefficient and ρ the crystal density) increases from (600–800)$\times10^{-15}$ s^3/kg for linearly polarized optical waves up to 1200×10^{-15} s^3/kg for circularly polarized optical waves. This occurs when the incident and diffracted optical beams propagate in the vicinity of the optic axis. Another example is optically active α-HIO_3 crystals. Here the AO efficiency also increases significantly when the incident and diffracted optical waves propagate along the directions close to the optic axis [5]. In the work [3], we have considered theoretically and experimentally a further example of $Pb_5Ge_3O_{11}$ crystals. It has been demonstrated that the AO efficiency can be enhanced for all the types of AO interactions. Finally, the study [6] has proved that the AO efficiency can be increased not only in naturally gyrotropic crystals but also in optically non-active crystalline materials due to a magnetically induced Faraday rotation. In the present work we will concentrate on commonly known optically active α-SiO_2 crystals.

Crystalline quartz is a well known material which is used in optics and optoelectronics due to its wide range of optical transparency, high optical homogeneity, high optical-damage threshold and low thermal expansion [7]. Different optical elements such as wedges, prisms, optical windows and lenses are produced from fused silica. Moreover, quartz is one of the most efficient piezoelectric crystalline materials that finds its applications in many devices such as piezoelectric resonators, oscillators, quartz clocks, etc. [8–10]. The AO devices fabricated on the basis of quartz crystals include, e.g., bulk and integrated optical modulators [11, 12] and tunable filters [13]. The AO modulators on α-SiO_2 can be operated at the optical wavelengths ranging from ultraviolet to near-infrared light (250–2500 nm), with the central AW frequency belonging to range 40–500 MHz [14]. However, the AW power required for the quartz-based AO devices is high enough and varies from 1 to 20 W [14]. This is due to a low AO figure of merit ($(1.48–2.38)\times10^{-15}$ s^3/kg [15]) peculiar for the case of AO interactions with longitudinal AWs, which follows from high enough AW velocities ($\sim 6\times10^3$ m/s). On the other hand, high AW velocities imply a kind of advantage of the AO devices. This provides a high repetition rate which is one of the most important parameters for Q-switched lasers [16].

The aim of the present work is to show how one can enlarge the AO figure of merit of the SiO_2 crystals due to its natural optical activity.

2. Method of analysis

α-SiO_2 crystals belong to the point symmetry group 32. They can exist in two enantiomorphous modifications that differ by their signs of optical rotation. The crystals are optically active, with the specific rotation equal to $\rho = 18.8$ deg/ mm at the optical wavelength $\lambda = 632.8$ nm [17]. The gyration tensor components at this wavelength are equal to $g_{33} = 10.06 \pm 0.07\times10^{-5}$ and $g_{11} = -4.8 \pm 0.5\times10^{-5}$ for a dextrorotary modification of the crystals [18]. The refractive indices amount to $n_o = 1.543$ and $n_e = 1.552$ [15]. The components p_{ijkl} of the EO tensor at $\lambda = 538$ nm are as follows: $p_{11} = 0.16$, $p_{13} = 0.27$, $p_{12} = 0.27$, $p_{14} = -0.030$, $p_{31} = 0.29$, $p_{33} = 0.10$, $p_{41} = -0.047$ and $p_{44} = -0.079$ (it is supposed that the dispersion of EO coefficients in the region 538–632.8 nm is week enough). The elastic stiffnesses C_{mnkl} are given by $C_{11} = 87.486$, $C_{33} = 107.2$, $C_{12} = 6.244$, $C_{13} = 11.91$, $C_{44} = 57.98$, $C_{66} = 40.626$ and $C_{14} = -18.09$ GPa [19, 20]. All of these coefficients have been measured under the condition of constant electric induction. Finally, the density of α-SiO_2 amounts to $\rho = 2649$ kg/m^3.

The Z and X axes of the optical indicatrix for α-SiO_2 are parallel respectively to the three-fold and two-fold symmetry axes. In our analysis, we will consider AO interactions between the optical waves and the quasi-longitudinal (QL) or quasi-transverse (QT) AWs in the YZ plane. Let us notice that the eigenvectors of the Christoffel tensor in the YZ plane are rotated only about the X axis so that the solutions for the eigenvalues of this tensor can be obtained analytically. It is not so for the XZ plane. We do not consider the interaction plane XY since the ellipticity of optical eigenwaves in this plane is negligibly small, even though the AO figure of merit for the isotropic AO interactions of the QL AW with the n_e-polarized optical waves in this plane acquires a maximum value, 2.38×10^{-15} s^3/kg [15].

The ellipticity of the optical eigenwaves is given by the relation [21]

$$\chi = \frac{1}{2G(\phi)}\left((n_o^2 - n'^2_e) - \sqrt{(n_o^2 - n'^2_e) + 4G(\phi)^2}\right) \approx \frac{G(\phi)}{n_o^2 - n'^2_e}, \quad (1)$$

where G is the scalar gyration parameter and ϕ the angle between the Z axis and the propagation direction of the incident optical wave. Note that the parameter

$$G(\phi) = g_{33}\sin^2\phi + g_{11}\cos^2\phi \quad (2)$$

and the refractive index

$$n'^2_e = \frac{n_o^2 n_e^2}{n_e^2\cos^2\phi + n_o^2\sin^2\phi} \quad (3)$$

depend on the propagation direction of the incident optical wave. The angle between the incident and diffracted optical waves has been taken to be small enough (0.2 deg) and the Bragg angle is equal to 0.1 deg. Then we have $\phi = \theta + \theta_B$, where θ is the angle between the Y axis and the wavevector of the AW in the YZ plane, while θ_B denotes the Bragg angle. The frequency and the velocity of the QL AW are equal respectively to $f_a = 49.8$ MHz and $v_{22} = 6022$ m/s at $\theta_B = 0.1$ deg, where the v_{ij} indices indicate the directions of AW propagation (i) and polarization (j). If we consider the QT AWs with the velocities v_{23} and v_{21}, the AW frequencies should be equal respectively to 35.7 and 32.7 MHz at the same condition.

The AW velocities can be obtained on the basis of a Christoffel equation:

$$v_{22}^{QL} = \sqrt{\frac{(C_{11}+C_{44})\cos^2\theta + (C_{44}+C_{33})\sin^2\theta - \sin 2\theta C_{14}}{2\rho} + \frac{\sqrt{\left\{(C_{11}-C_{44})\cos^2\theta + (C_{44}-C_{33})\sin^2\theta - \sin 2\theta C_{14}\right\}^2 + 4\left\{0.5\sin 2\theta(C_{13}+C_{44}) - C_{14}\cos^2\theta\right\}^2}}{2\rho}}, \quad (4)$$

$$v_{21}^{QT_2} = \sqrt{\frac{C_{66}\cos^2\theta + C_{44}\sin^2\theta + \sin 2\theta C_{14}}{\rho}}, \quad (5)$$

$$v_{23}^{QT_1} = \sqrt{\frac{(C_{11}+C_{44})\cos^2\theta + (C_{44}+C_{33})\sin^2\theta - \sin 2\theta C_{14}}{2\rho} - \frac{\sqrt{\left\{(C_{11}-C_{44})\cos^2\theta + (C_{44}-C_{33})\sin^2\theta - \sin 2\theta C_{14}\right\}^2 + 4\left\{0.5\sin 2\theta(C_{13}+C_{44}) - C_{14}\cos^2\theta\right\}^2}}{2\rho}}. \quad (6)$$

The angle of deviation from the purely longitudinal polarization state for the QL AW reads as

$$\zeta_1 = \theta - 0.5\arctan\frac{(C_{13}+C_{44})\sin 2\theta - 2C_{14}\cos^2\theta}{(C_{11}-C_{44})\cos^2\theta + (C_{44}-C_{33})\sin^2\theta - C_{14}\sin 2\theta}. \quad (7)$$

Note that this angle defines the rotation of the coordinate eigensystem of the Christoffel tensor around the X axis. The QT_2 AW is a purely transverse wave. The effective EO coefficients for the types I and II of AO interactions (i.e., the isotropic AO interactions of the n_o- and n_e-polarized optical waves with the QL AW) are as follows:

$$p_{eff}^{2(I)}=\left(p_{12}\cos\theta\cos\zeta_1+p_{13}\sin\theta\sin\zeta_1\right)^2 +\chi^2\begin{pmatrix}\left(p_{11}\cos\theta\cos\zeta_1+p_{13}\sin\theta\sin\zeta_1-p_{14}\sin(\zeta_1+\theta)\right)^2\cos^4\theta\\ +\left(p_{31}\cos\theta\cos\zeta_1+p_{33}\sin\theta\sin\zeta_1\right)^2\sin^4\theta+0.5\left(p_{44}\sin(\zeta_1+\theta)\right)^2\sin^2 2\theta\\ +\left(p_{11}\cos\theta\cos\zeta_1+p_{13}\sin\theta\sin\zeta_1-p_{14}\sin(\zeta_1+\theta)\right)\\ \times\left(p_{44}\sin(\zeta_1+\theta)\right)\sin 2\theta\cos^2\theta\\ +\left(p_{44}\sin(\zeta_1+\theta)\right)\\ \times\left(p_{31}\cos\theta\cos\zeta_1+p_{33}\sin\theta\sin\zeta_1\right)\sin 2\theta\sin^2\theta\end{pmatrix}, \quad (8)$$

$$\begin{aligned}p_{eff}^{2(II)}=&\cos^2(\theta_B+\theta)\begin{bmatrix}(p_{11}\cos\theta\cos\zeta_1+p_{13}\sin\theta\sin\zeta_1-p_{14}\sin(\zeta_1+\theta))^2\cos^2\theta\\ +(p_{44}\sin(\zeta_1+\theta)-p_{41}\cos\theta\cos\zeta_1)^2\sin^2\theta\end{bmatrix}\\ &+(p_{44}\sin(\zeta_1+\theta)-p_{41}\cos\theta\cos\zeta_1)\sin 2(\theta_B+\theta)\\ &\times\begin{bmatrix}(p_{11}\cos\theta\cos\zeta_1+p_{13}\sin\theta\sin\zeta_1-p_{14}\sin(\zeta_1+\theta))\cos^2\theta\\ +(p_{31}\cos\theta\cos\zeta_1+p_{33}\sin\theta\sin\zeta_1)\sin^2\theta\end{bmatrix}\\ &+\sin^2(\theta_B+\theta)\begin{bmatrix}(p_{44}\sin(\zeta_1+\theta)-p_{41}\cos\theta\cos\zeta_1)^2\cos^2\theta\\ +(p_{31}\cos\theta\cos\zeta_1+p_{33}\sin\theta\sin\zeta_1)^2\sin^2\theta\end{bmatrix}\\ &+\chi^2\left[(p_{12}\cos\theta\cos\zeta_1+p_{13}\sin\theta\sin\zeta_1+p_{14}\sin(\zeta_1+\theta))^2\right].\end{aligned} \quad (9)$$

The relations for the types III and IV of isotropic AO diffraction of the n_o- and n_e-polarized optical waves by the QT_1 AW are given by

$$p_{eff}^{2(III)}=\left(p_{13}\sin\theta\cos\zeta_1-p_{12}\cos\theta\sin\zeta_1+p_{14}\cos(\zeta_1+\theta)\right)^2 +\chi^2\begin{pmatrix}\left(p_{13}\sin\theta\cos\zeta_1-p_{11}\cos\theta\sin\zeta_1-p_{14}\cos(\zeta_1+\theta)\right)^2\cos^4\theta\\ +\left(p_{33}\sin\theta\cos\zeta_1-p_{31}\cos\theta\sin\zeta_1\right)^2\sin^4\theta\\ +0.5\left(p_{41}\sin\theta\cos\zeta_1+p_{44}\cos(\zeta_1+\theta)\right)^2\sin^2 2\theta\\ +\left(p_{13}\sin\theta\cos\zeta_1-p_{11}\cos\theta\sin\zeta_1-p_{14}\cos(\zeta_1+\theta)\right)\\ \times\left(p_{41}\sin\theta\cos\zeta_1+p_{44}\cos(\zeta_1+\theta)\right)\sin 2\theta\cos^2\theta\\ +\left(p_{41}\sin\theta\cos\zeta_1+p_{44}\cos(\zeta_1+\theta)\right)\\ \times\left(p_{33}\sin\theta\cos\zeta_1-p_{31}\cos\theta\sin\zeta_1\right)\sin 2\theta\sin^2\theta\end{pmatrix}, \quad (10)$$

$$\begin{aligned}p_{eff}^{2\,(IV)}=&\cos^2(\theta_B+\theta)\begin{bmatrix}(p_{13}\sin\theta\cos\zeta_1-p_{11}\cos\theta\sin\zeta_1-p_{14}\cos(\zeta_1+\theta))^2\cos^2\theta\\ +(p_{44}\cos(\zeta_1+\theta)+p_{41}\cos\theta\sin\zeta_1)^2\sin^2\theta\end{bmatrix}\\ &+(p_{44}\cos(\zeta_1+\theta)+p_{41}\cos\theta\sin\zeta_1)\sin 2(\theta_B+\theta)\\ &\times\begin{bmatrix}(p_{13}\sin\theta\cos\zeta_1-p_{11}\cos\theta\sin\zeta_1-p_{14}\cos(\zeta_1+\theta))\cos^2\theta\\ +(p_{33}\sin\theta\cos\zeta_1-p_{31}\cos\theta\sin\zeta_1)\sin^2\theta\end{bmatrix}\\ &+\chi^2\sin^2(\theta_B+\theta)\begin{bmatrix}(p_{44}\cos(\zeta_1+\theta)+p_{41}\cos\theta\sin\zeta_1)^2\cos^2\theta\\ +(p_{33}\sin\theta\cos\zeta_1-p_{31}\cos\theta\sin\zeta_1)^2\sin^2\theta\end{bmatrix}\\ &+(p_{13}\sin\theta\cos\zeta_1-p_{12}\cos\theta\sin\zeta_1+p_{14}\cos(\zeta_1+\theta))^2.\end{aligned} \quad (11)$$

Finally, the isotropic types V and VI of AO diffraction of the n_o- and n_e-polarized optical waves by the QT_2 AW can be described by the relations

$$p_{eff}^{2(\mathrm{V})} = p_{14}^2 \sin^2\theta + 0.25\chi^2 \left((p_{44}^2 \sin^2\theta - p_{14}^2 \cos^2\theta)\sin^2 2\theta - p_{44}p_{14}\sin^3 2\theta \right), \quad (12)$$

$$p_{eff}^{2(\mathrm{VI})} = \left(p_{44}^2 \sin^4\theta - 0.25 p_{14}^2 \sin^2 2\theta \right)\cos^2(\theta_B + \theta) + 0.25 p_{44}^2 \sin^2(\theta_B + \theta)\sin^2 2\theta$$
$$-0.25 p_{14}p_{44}\sin 2(\theta_B + \theta)\sin^2 2\theta + \chi^2 p_{14}^2 \sin^2\theta. \quad (13)$$

3. Results and their discussion

Cross-sections of the AW-velocity surfaces by the principal planes of the principal coordinate system *XYZ* are shown in Fig. 1. As seen from Fig. 1a, b, the acoustic axis is parallel to the *Z* direction. The transverse AWs with orthogonal polarizations propagate with the same velocity along the acoustic axis. It is known that the orientation of this axis is determined by the crystal symmetry [22]. The velocities of the QT waves with orthogonal polarizations, which propagate at the angles 33 and 147 deg with respect to the *X* axis, differ by about 156 m/s (Fig. 1a). Hence, the above directions cannot be classified as the acoustic axes. The direction in the *YZ* plane (see Fig. 1b), which is given by the angle 157 deg with respect to the *Y* axis, does not represent the acoustic axis since the difference in the velocities of the QT AWs is nonzero (~ 20 m/s). Finally, there are no acoustic axes in the *XY* plane (see Fig. 1c).

Fig. 2 shows a dependence of the angle of deviation of the QL and QT_1 AW-polarizations from the purely longitudinal or transverse states on the wavevector direction in the *YZ* plane. This angle is equal to zero for the directions defined by $\theta = 40.5, 90.0, 107.5$ and 162 deg and reaches its maximal values, 20.0 and –26.3 deg, respectively at $\theta = 150$ and 175 deg.

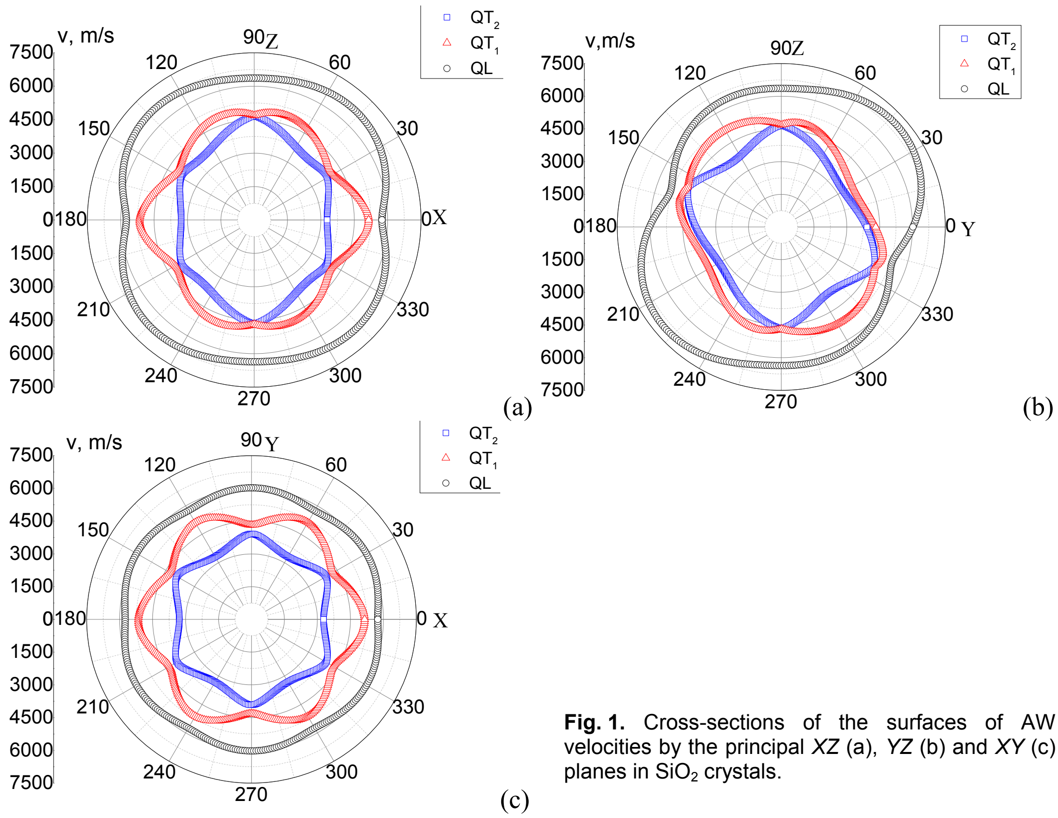

Fig. 1. Cross-sections of the surfaces of AW velocities by the principal *XZ* (a), *YZ* (b) and *XY* (c) planes in SiO_2 crystals.

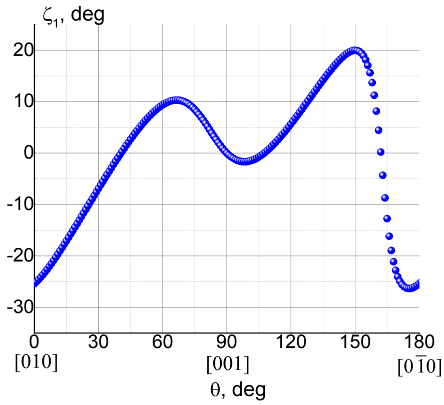

Fig. 2. Dependence of the angle of deviation from the purely longitudinal (or purely transverse) polarization states on the wavevector direction in the *YZ* plane, as calculated for the QL AW.

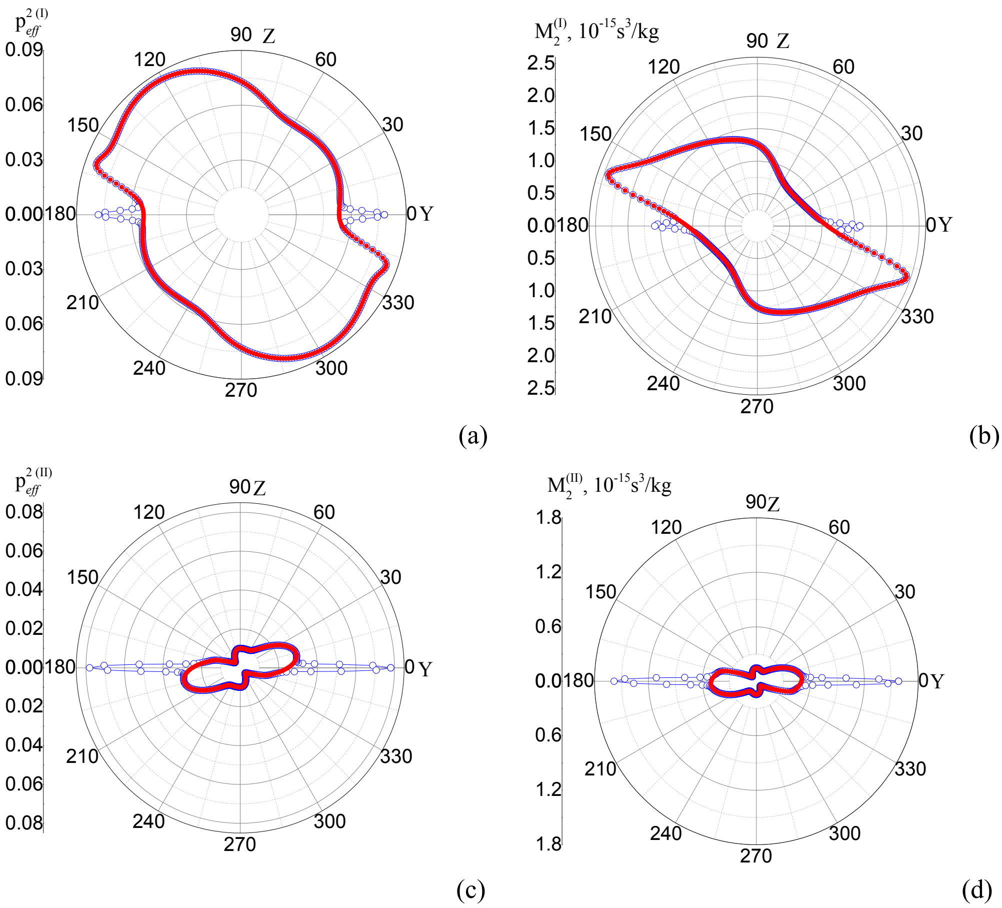

Fig. 3. Dependences of squared effective EO coefficient (a, c) and AO figure of merit (b, d) on the angle θ for AO interactions of the type I (a, b) and type II (c, d): full circles correspond to disregard of the eigenwave ellipticity and open circles to consideration of this ellipticity.

As seen from Fig. 3, the effective EO coefficient and the AO figure of merit for the type I of AO interactions increases when the incident and diffracted optical waves propagate in a narrow vicinity of the optic axis. This is due to accounting for the ellipticity of optical eigenwaves, which is caused by the natural optical activity. These directions correspond to AW propagation nearly parallel to the Y axis ($\theta \approx 0$). At the type I of AO interactions of the n_o-polarized optical waves with the QL AW, the effective EO coefficient increases from 0.23 up to the value 0.28 (see Fig. 3a). This increases the AO figure of merit from 1.08×10^{-15} s^3/kg to 1.58×10^{-15} s^3/kg (see Fig. 3b). The full width at half maximum (FWHM) of the peak of AO figure of merit is equal to ~ 4 deg. Note that the FWHM parameter indicates the angular region θ in which a peak-like increment of the AO figure of merit is not less than a half of its maximal value. At the type II of AO interactions of the n_e-polarized optical waves with the QL AW, the effective EO coefficient increases from 0.16 up to 0.28, while the AO figure of merit increases from 0.50×10^{-15} to 1.58×10^{-15} s^3/kg. Here the FWHM of peak of the AO figure of merit is also equal to ~ 4 deg.

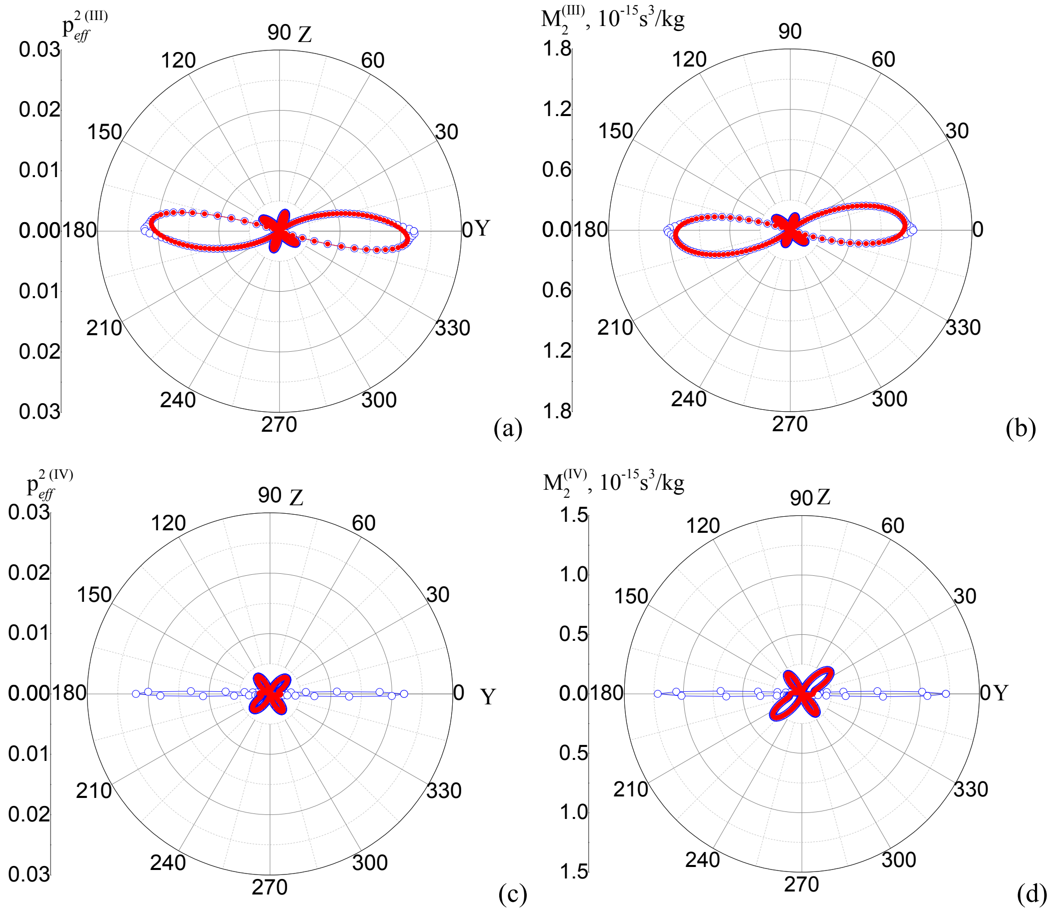

Fig. 4. Dependences of squared effective EO coefficient (a, c) and AO figure of merit (b, d) on the angle θ for AO interactions of the type III (a, b) and type IV (c, d) with the QT_1 AW: full circles correspond to disregard of the eigenwave ellipticity and open circles to consideration of this ellipticity.

The increase in the effective EO coefficient and the AO figure of merit, which is associated with a nonzero ellipticity of optical eigenwaves, is also observed for the types III and IV of AO interactions with the QT_1 AW (see Fig. 4). In case of the type III of AO interactions, the AO figure of merit increases from 1.12×10^{-15} up to 1.22×10^{-15} s^3/kg (see Fig. 4b). The FWHM of the peak of the AO figure of merit is equal to ~ 4 deg. Consideration of the type IV of AO interactions of the n_e-polarized optical waves with the QT_1 AW testifies that the peaks of the effective EO coefficient and the AO figure of merit are significant (see Fig. 4c, d). The AO figure of merit increases by more than order of magnitude, from 9.6×10^{-17} to 1.22×10^{-15} s^3/kg and the appropriate FWHM amounts to ~ 4 deg (see Fig. 4d).

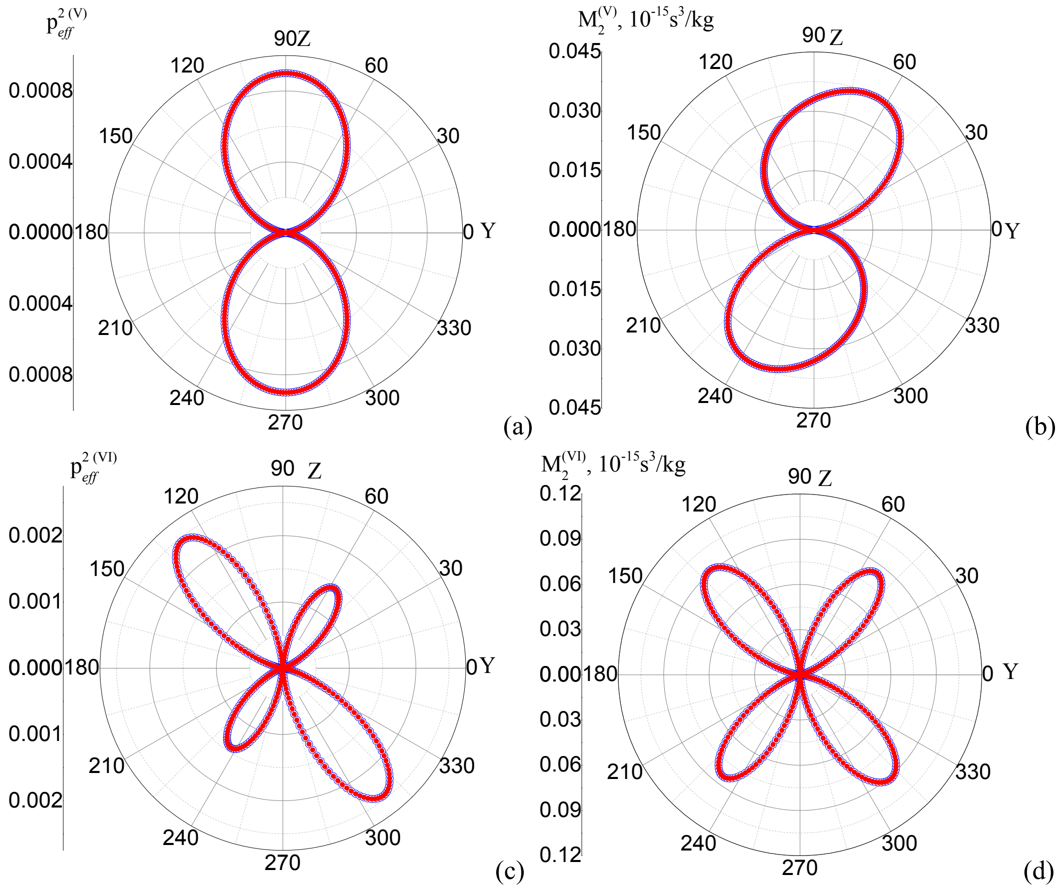

Fig. 5. Dependences of squared effective EO coefficient (a, c) and AO figure of merit (b, d) on the angle θ for AO interactions of the type V (a, b) and type VI (c, d) with the QT_2 AW: full circles correspond to disregard of the eigenwave ellipticity and open circles to consideration of this ellipticity.

For the types V and VI of AO interactions with the QT_2 AW, no increase in the effective EO coefficients and the AO figure of merit is observed due to accounting for the ellipticity of optical eigenwaves (see Fig. 5). Indeed, it is seen from Eqs. (12) and (13) that the effective EO coefficients for these types of interactions are equal to zero at $\theta = 0$.

Using the type II of AO interactions as an example, we have studied the dependence of the increment of the AO figure of merit on the AW frequency. It is seen from Fig. 6 that the increase in the AW frequency from 49.8 MHz to 1 GHz shifts the increment peak by ~ 3 deg. At the same time, the height of the peak increases slightly (from 1.08×10^{-15} to 1.13×10^{-15} s^3/kg). The above angular shift is explained by a dependence of the Bragg angle on the AW frequency, as well as dependences of the extraordinary refractive index, the ellipticity of optical eigenwaves and the effective EO coefficient on the Bragg angle (see Eqs. (1)–(3) and (9)). Note that we have the angle $\phi < 1.9$ deg at half of the FWHM angle (~ 2 deg) and the Bragg angle larger than 0.1 deg. With such a small incidence angle with respect to the *Z* axis, the ellipticity of optical eigenwave is higher than 0.96. In other terms, it is not necessary to align the polarization of the incident optical wave with that of the elliptically polarized eigenwave. One can use the incident circular polarized wave instead.

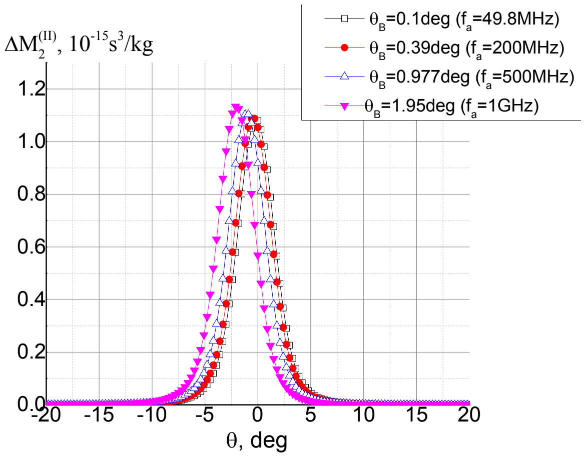

Fig. 6. Dependences of increments of the AO figure of merit for the type II of AO interactions, as found for different AW frequencies.

Finally, let us consider the efficiency of AO diffraction, which is given by the relation $\eta = I_d / I_0 \approx \left(\pi^2 L / 2H\lambda^2 \cos^2\theta_B\right) M_2 P_a$, where I_0 and I_d are the intensities of respectively the incident and diffracted optical waves, λ denotes the wavelength of optical radiation in vacuum, L the AO-interaction length, H the height of the acoustic beam, and P_a the AW power. Our results demonstrate that the efficiency of AO diffraction can be increased when the AWs interact with elliptically (or circularly) polarized optical waves in the quartz crystals. For example, the AW power needed for reaching a given AO diffraction efficiency can be reduced by three times in case of the type II of AO interactions. Moreover, the peak value of the AO figure of merit can be enhanced by ~ 19% (i.e., up to 1.22×10^{-15} s^3/kg) at the III type of AO interactions.

Besides, we have revealed a new promising geometry of AO interactions in the quartz crystals, which is due to accounting for the ellipticity of optical eigenwaves. It is the isotropic interaction of the n_e-polarized optical wave with the QT_1 AW propagating in the vicinity of the Y axis (i.e., the type IV of AO interactions). Thanks to a nonzero optical-eigenwave ellipticity, the AO figure of merit then increases from nearly zero value to 1.22×10^{-15} s^3/kg. Although the AO figure of merit at the types II, III and IV of AO interactions increases notably in the case when the ellipticity of eigenwaves is taken into account, it is still less than the value 2.38×10^{-15} s^3/kg achieved for the case of AW propagation along the X axis and the AO interaction in the XY plane. The latter value is due to high enough EO coefficient, $p_{31} = 0.29$ [15].

4. Conclusion

In the present work, we have analyzed the influence of the natural optical activity on the efficiency of the isotropic AO diffraction in the quartz crystals. It has been found that, for the types I and II of AO interactions with the QL AW, the natural optical activity imposes a peak-like increase in the effective EO coefficients and the OA figure of merit. This occurs for the case of AO interactions with the optical eigenwaves. For the type I of AO interactions, the AO figure of merit increases by 54% up to the value $1.58\times10^{-15}$$s^3$/kg, while for the type II of interactions it increases more than three times and achieves the same value. A similar situation is typical for the types III and IV of AO interactions with the QT_1 AW. At the III type of AO interactions, the peak value of the AO figure of merit can be enhanced by 19% up to 1.22×10^{-15} s^3/kg, while the AO figure of merit for the type IV of AO interactions increases by more than order of magnitude (from 9.6×10^{-17} up to 1.22×10^{-15} s^3/kg).

Acknowledgement. The authors acknowledge the Ministry of Education and Science of Ukraine for financial support of the present study (the Project #0123U101781).

References

1. Kharusai M S and Farnell G W, 1969. Observation of optical activity in Brillouin scattering experiments. Canad. J. Phys. **47**: 2719–2725.
2. Belyi V N, Kazak N S and Kulak G V, 2000. Features of acousto-optic interaction in uniaxial gyrotropic crystals. J. Appl. Spectr. **67**: 139–147.
3. Mys O, Kostyrko M, Adamenko D, Martynyuk-Lototska I, Skab I and Vlokh R, 2022. Effect of ellipticity of optical eigenwaves on the enhancement of efficiency of acousto-optic Bragg diffraction. A case of optically active $Pb_5Ge_3O_{11}$ crystals. AIP Adv. **12**: 055130.
4. Yano T and Watanabe A, 1974. Acousto-optic figure of merit of TeO_2 for circularly polarized light. J. Appl. Phys. 1243–1245.
5. Kurpeychik M I and Balakshy V I, 2018. Peculiarities of acousto-optic interaction in biaxial crystal of alpha-iodic acid. Appl. Opt. **57**: 5549–5555.
6. Mys O, Adamenko D and Vlokh R, 2023. Influence of Faraday elliptical birefringence on the acousto-optic diffraction efficiency: a case of isotropic interaction with quasi-longitudinal acoustic waves in KH_2PO_4 crystals. Ukr. J. Phys. Opt. **24**: 95–103.
7. Moore L A and Smith C M, 2022. Fused silica as an optical material. Opt. Mater. Express. **12**: 3043–3059.
8. Cady W G, 1921. The piezoelectric resonator. Phys. Rev. **17**: 531.
9. Pierce G W, 1923. Piezoelectric crystal resonators and crystal oscillators applied to the precision calibration of wavemeters. Proc. Amer. Acad. Arts Sci. **59**: 81–106.
10. Lombardi M, 2008. The accuracy and stability of quartz watches. Horol. J.: 57–59.
11. Khorsheed S M and Yaseen N M, 2021. Effect of square shaped acousto-optic modulators on the Bragg diffraction. J. Phys.: Conf. Ser. **1897**: 012074
12. Pitt C W, Skinner J D and Townsend P D, 1984. Acousto-optic diffraction of optical guided waves in crystal quartz. Electron. Lett. **20**: 4–5.
13. Chang I C, 1974. Tunable acoustooptic filter utilizing acoustic beam walkoff in crystal quartz. Appl. Phys. Lett. **25**: 323–324.
14. https://www.gophotonics.com/search/acousto-optic-modulator/filters?page=1&country=global&sacousto_optic_material=;Quartz%20Crystal.
15. Shaskolskaya M P. Acoustic Crystals. Moscow: Nauka, 1982.
16. Di Wang, Jia Zhao, Kejian Yang, Shengzhi Zhao, Tao Li, Dechun Li, Guiqiu Li and Wenchao Qiao, 2016. Modulation frequency characteristics in a doubly Q-switched $Nd:Gd_{0.63}Y_{0.37}VO_4$ laser with an acoustooptic modulator and a V^{3+}:YAG saturable absorber. Opt. Quant. Electron. **48**: 553.
17. Collins R W and Ferlauto A S, 2005. Optical physics of materials, in: Irene E G & Tomkins H G (Eds), Handbook of Ellipsometry. Norwich, NY: William Andrew.
18. Arteaga O, Canillas A and Jellison G E Jr, 2009. Determination of the components of the gyration tensor of quartz by oblique incidence transmission two-modulator generalized ellipsometry. Appl. Opt. **48**: 5307–5317.
19. Narasimhamurty T S, 1969. Photoelastic constants of a quartz. J. Opt. Soc. Amer. **59**: 682–686.

20. Landolt-Borstein. Zahlenwerte und Funktionen aus Naturwissenschaften und Technik. Neue Serie: Bd. I. Elastiche, piezooptishe konstanten von kristallen. Berlin: Springer, 1971.
21. Konstantinova A F, Grechushnikov B N, Bokut B V and Valyashko E G. Optical Properties of Crystals. Minsk: Navuka i Tekhnika, 1995.
22. Sirotin Yu and Shaskolskaya M P. Fundamentals of Crystal Physics. Moscow: Nauka, 1975.

Mys O., Adamenko D. and Vlokh R. 2023. Enhancement of acousto-optic diffraction efficiency in SiO_2 crystals due to ellipticity of optical eigenwaves: isotropic acousto-optic interaction. Ukr.J.Phys.Opt. 24: 124 – 134. doi: 10.3116/16091833/24/2/124/2023

Анотація. *На основі аналізу впливу природної оптичної активності на ефективність ізотропної акустооптичної (АО) дифракції встановлено, що врахування оптичної активності та ненульової еліптичності власних оптичних хвиль у кристалах кварцу приводить до пікоподібного зростання ефективних пружнооптичних коефіцієнтів і АО-добротності. Показано, що АО-добротність для типу I взаємодій зростає на 54%, досягаючи значення* $1{,}58\times10^{-15}$ $с^3$*/кг. За типу II взаємодій, АО-добротність зростає більш ніж у тричі та досягає приблизно такого ж значення. Подібна ситуація має місце і для типів III і IV АО-взаємодій із акустичною хвилею* QT_1*. Зокрема, пікове значення АО-добротності для типу III взаємодій зростає на 19% і досягає* $1{,}22\times10^{-15}$ $с^3$*/кг, тоді як АО-добротність для типу IV взаємодій зростає більш ніж на порядок величини (від* $9{,}6\times10^{-17}$ *до* $1{,}22\times10^{-15}$ $с^3$*/кг). Результати нашого дослідження можуть бути корисними для розробки АО-приладів на основі кристалічного кварцу та для мінімізації їхнього енергоспоживання.*

Ключові слова: *акустооптична дифракція, оптична активність, кристали кварцу, дифракційна ефективність, еліптичність оптичних власних хвиль*